

Chapter 23

Nonlinear Finite Element Model Updating, Part I: Experimental Techniques and Nonlinear Modal Model Parameter Extraction

Benjamin R. Pacini, Randall L. Mayes, Brian C. Owens, and Ryan A. Schultz

Abstract Linear structural dynamic models are often used to support system design and qualification. Overall, linear models provide an efficient means for conducting design studies and augmenting test data by recovering un-instrumented or un-measurable quantities (e.g. stress). Nevertheless, the use of linear models often adds significant conservatism in design and qualification programs by failing to capture critical mechanisms for energy dissipation. Unfortunately, the use of explicit nonlinear models can require unacceptably large efforts in model development and experimental characterization to account for common nonlinearities such as frictional interfaces, macro-slip, and other complex material behavior. The computational requirements are also greater by orders of magnitude. Conversely, modal models are much more computationally efficient and experimentally have shown the ability to capture typical structural nonlinearity. Thus, this work will seek to use modal nonlinear identification techniques to improve the predictive capability of a finite element structural dynamics model.

Part I of this paper discusses the experimental aspects of this work. Linear natural frequencies, damping values, and mode shapes are extracted from low excitation level testing. Subsequently, the structure is excited with high level user-defined shaker inputs. The corresponding response data are modally filtered and fit with nonlinear elements to create the nonlinear pseudo-modal model. This is then used to simulate the measured response from a high level excitation experiment which utilized a different type of input. The nonlinear model is then employed in a reduced order, generalized structural dynamics model as discussed in Part II.

Keywords Nonlinear System Identification • Nonlinear Simulation • Structural Dynamics • Modal Model • Restoring Force Surface

Abbreviations

a	Time history of the triangle function
c	Damping coefficient
f	Frequency in cycles/sec
f_c	Center frequency in cycles/sec
F	Force
F_r	Restoring force
G_{vf}	Shaker voltage to excitation force transfer function
j	Imaginary number variable
k	Stiffness coefficient
q	Modal degree of freedom
t	Time

Sandia National Laboratories is a multi-program laboratory managed and operated by Sandia Corporation, a wholly owned subsidiary of Lockheed Martin Corporation, for the U.S. Department of Energy National Nuclear Security Administration under Contract DE-AC04-94AL85000.

B.R. Pacini
Sandia National Laboratories, PO Box 5800, 87185, Albuquerque, NM, USA
e-mail: brpacin@sandia.gov

R.L. Mayes (✉) • B.C. Owens • R.A. Schultz
Structural Dynamics Department, Sandia National Laboratories, P.O. Box 5800 – MS0557, Albuquerque, NM 87185, USA
e-mail: rlmayes@sandia.gov; bcowens@sandia.gov; rschult@sandia.gov

t_r	Rise time
x	Physical displacement degree of freedom
v, V	Shaker voltage, time domain and frequency domain, respectively
ζ	Modal damping ratio
ω	Frequency in radians per second
φ_{dp}	Drive point mode shape value
\mathbf{H}	Frequency response function matrix
\mathbf{P}	Modal response matrix
$\underline{\mathbf{U}}$	Known restoring force vector
$\underline{\Psi}$	Modal filter vector
D	Subscript for desired
flm	Subscript for “first local minimum”
\mathcal{F}	Subscript for Fourier transform
lin	Subscript for linear
n	Subscript for natural
nl	Subscript for nonlinear
u	Subscript for updated
$+$	Moore-Penrose pseudo-inverse of a matrix

23.1 Introduction and Motivation

A large class of structural dynamic system responses are mildly nonlinear in stiffness (a few percent modal frequency change) and significantly nonlinear in damping (hundreds of percent damping ratio change) as a function of amplitude of vibration. We desire to experimentally identify such a system and then simulate the nonlinear response analytically. Such systems will typically be linear at low level excitation. At higher levels of excitation, the resonant frequencies typically decrease slightly and the apparent damping can increase more than 100%. Structures with joints typically have this softening behavior. Low-excitation-level linear models used to simulate the response may over-predict the nonlinear response by tens to hundreds of percent. Consider a frequency response function (FRF) from the hardware used in this work due to a high level and a low level impact as shown in Fig. 23.1. The low level FRF peak is almost a factor of two greater than the high level FRF peak. Occasionally, the resonant frequency will slightly increase and the apparent damping decrease as forcing amplitude increases. We desire to be able to simulate both softening and stiffening behavior.

There are two main analytical methods to capture the nonlinear behavior: local physical models and pseudo-modal models. The former are extremely computationally expensive and are prohibitively difficult to experimentally identify on a complex structure. The latter assumes the total system response of a structure is a superposition of the responses of individual modes. This allows one to study each mode individually and apply nonlinear elements in parallel with the linear spring and damper.

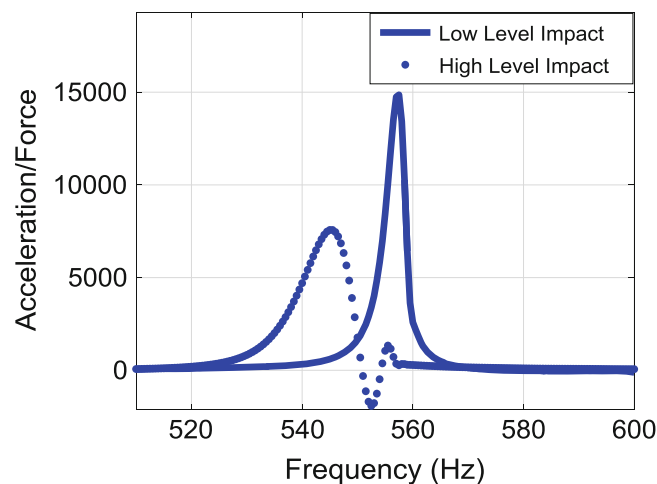


Fig. 23.1 Drive point FRF – low level vs high level impact force

Inherent in this approach is the assumption that the mode shapes do not change with response amplitude, and that the modal degrees of freedom (DOF) do not interact. The pseudo-modal approach is computationally inexpensive and methods have been developed which allow for the extraction of parameters for nonlinear models. Therefore, the pseudo modal approach is utilized for this work.

The methodology used here follows that of [1] which used the pseudo-modal model to characterize the nonlinearities of a complex structure via three different nonlinear elements/identification methodologies. The Restoring Force Surface (RFS) technique described in that work is the nonlinear model structure/identification method employed here. The approach begins with the standard modal model using a linear spring and damper for each modal mass. The spring and damper are identified in a standard low-level modal test. Then we assume that, for the nonlinear modes, nonlinear elements can be connected in parallel with the standard linear elements. Unlike the previous work using impact testing, this work shows the advantages of high level shaker tests on the nonlinear structure to provide calibration data for fitting the nonlinear parameters. The identification of these parameters is accomplished using a single modal single degree of freedom (SDOF) response created by modally filtering the measured structural responses from the high level tests. The nonlinear elements are realized by cubic polynomials for stiffness and damping as a function of response amplitude.

In Sect. 23.3 the test hardware and instrumentation is described along with the new shaker testing approach that focuses the input force on the mode of interest. The modal filtering technique used in this work is presented in Sect. 23.4. Section 23.5 describes the nonlinear model and the parameter identification processes. In Sect. 23.6 the simulation results are compared against measured high level truth data utilizing a different forcing function than the calibration data, and observations are given. Section 23.7 provides conclusions. In Part II of the paper the experimental results are incorporated into the analytical modeling framework as an update to the finite element model.

23.2 Experiments

23.2.1 Hardware Description

A solid model cross-section of the test hardware, named the Cylinder-Plate-Beam assembly (CPB), is shown in Fig. 23.2 along with the coordinate systems (CS) utilized in this work. The physical hardware is shown in Fig. 23.3. The Beam is bolted and epoxied to the Plate. The Plate-Beam is then mounted on the forward flange of the Cylinder using eight bolts. All three components are 6061 T6 aluminum. Two coordinate systems were utilized for this test: a global Cartesian coordinate system and a cylindrical coordinate system. The zero degree orientation of the cylindrical CS aligns with the global CS (i.e. $\theta = 0^\circ$ aligns the cylindrical $R+$ with the Cartesian $X+$).

23.2.2 Test Set-Up

The CPB was softly suspended using two bungee cords to approximate a free-free boundary condition and instrumented with 10 and 100 mV/g accelerometers. Twenty-six triaxial and four uniaxial accelerometers were mounted at locations that were selected as a subset of the finite element model (FEM) nodes and minimized the condition number of the finite element mode shape matrix for the modes below 1600 Hz. By minimizing this condition number, the modal observability and independence of the mode shapes extracted from measured data were maximized.

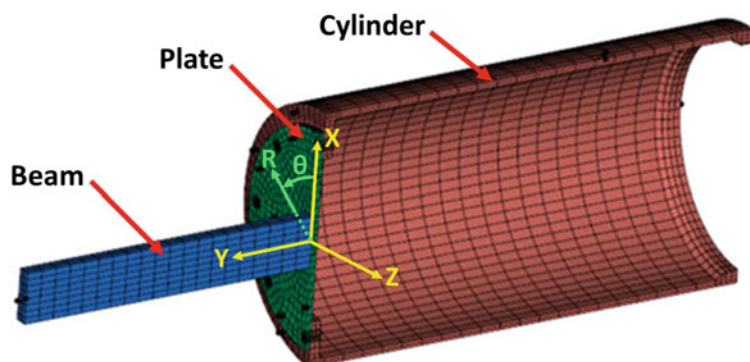


Fig. 23.2 Cylinder Plate Beam assembly full system solid model and coordinate systems

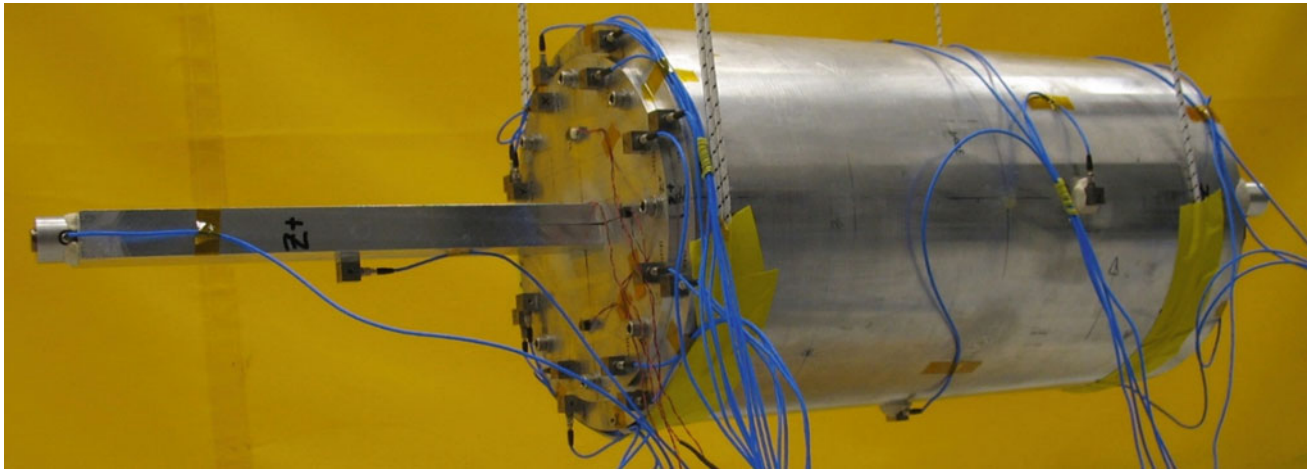


Fig. 23.3 Physical test hardware

Table 23.1 Excitation information, low-level tests

Input DOF	Description	Input type
34965R	Radial input on mid span of cylinder at 60°	Hammer
32916R	Radial input on mid span of cylinder at 30°	Hammer
53632Y	Axial input at tip of Beam	Shaker
25449Y	Axial input at aft end of cylinder at 270°	Shaker
31349Y	Axial input at aft end of cylinder at 0°	Shaker

23.2.3 Test Procedure

A series of tests were performed in this work. The first was to conduct low-level excitation tests in order to establish a linear model and collect data for developing the modal filter. Subsequently, high-level excitation tests were conducted in order to collect data for calibration of parameters for the nonlinear pseudo-modal model.

23.2.4 Extraction of the Linear Modal Model

The linear model is an essential step in this work as its mode shape matrix allows for the translation between the physical and modal domains. Additionally, the modal filter is calculated from this step (see Sect. 23.4) as well as the linear coefficients of the pseudo-modal model (see Sect. 23.5).

Low-level excitation was input at the DOFs shown in Table 23.1 in order to extract linear modal parameters (natural frequencies, damping, and shapes) of the CPB. The input force was reduced as much as possible to minimize the nonlinear response of the CPB but remain sufficiently above the noise floor. A combination of hammer impact and low-level burst random tests were used to extract the linear parameters. The Synthesize Modes And Correlate (SMAC) program by Mayes and Hensley [2] was used to extract modal parameters from each data set individually using a real modes approximation in Table 23.2. Rigid body mode shapes were calculated from solid model mass properties.

The CPB contains only metal components that are bolted together. Thus the only significant source of nonlinearity in the amplitudes achieved in this work are the joints. The only modes that exhibit detectable nonlinear response are the bending modes (7, 8, and 14) and the axial mode (11). Therefore, only these modes were selected for nonlinear modeling.

Table 23.2 Linear modal parameters^{a, b}

Mode	f_n (Hz)	ζ (%cr)	Reference	Shape description
7	128	0.30	31349Y	First bend of Beam in soft direction (global X)
8	171	0.31	25449Y	First bend of Beam in stiff direction (global Z)
9	391	0.21	34965R	(2,0) ovaling of cylinder aligned with X-Z axes
10	395	0.03	34965R	(2,0) ovaling of cylinder 45° from X-Z axes
11	560	0.34	53632Y	Axial mode
12	957	0.11	34965R	(3,0) ovaling of cylinder
13	958	0.09	32916R	(3,0) ovaling of cylinder
14	978	0.23	31349Y	Second bend of Beam in soft direction (global X)

^aModes 7, 8, 11 and 14 were considered nonlinear

^bRigid body modes not shown

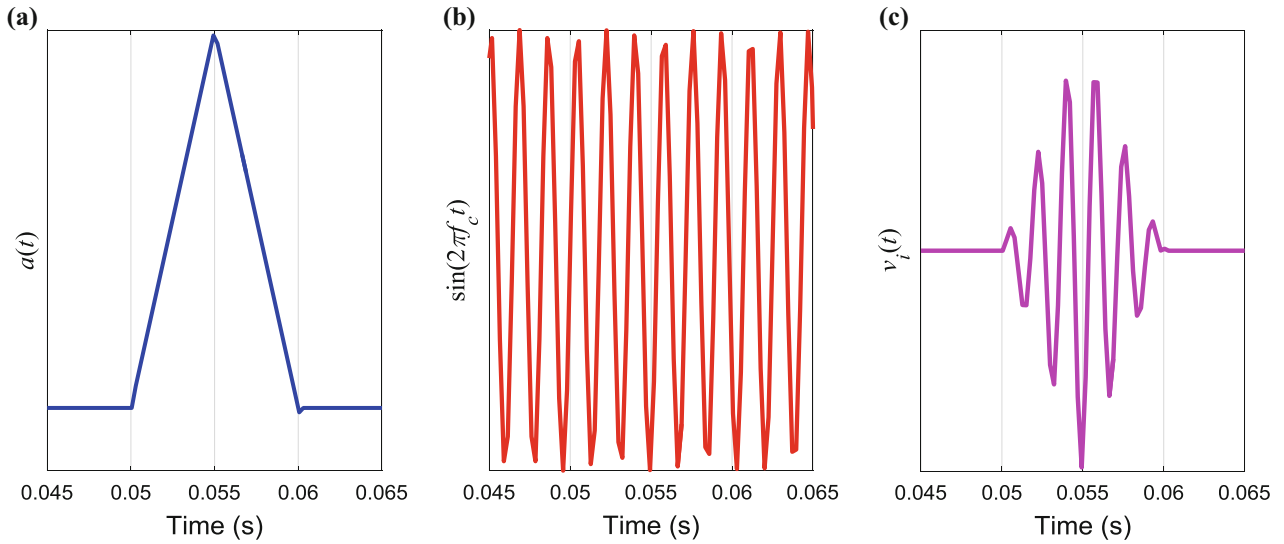


Fig. 23.4 Shaker input creation, time domain; (a) triangle wave $a(t)$, (b) sine wave $\sin(2\pi f_c t)$, and (c) combined signal $v_i(t)$

23.2.4.1 High Level Shaker Testing

Reference [1] utilized impact testing to extract parameters for the nonlinear models. However, impacts excite all modes at once, thus causing a large initial response which can overload accelerometers, especially the drive point. Therefore, this work employed shaker testing in order to increase the excitation amplitude of individually targeted nonlinear modes.

One method of nonlinear testing with a shaker involves a stepped-sine input with closed-loop control to maintain either constant force or response amplitude. This process is slow and difficult to practically implement due to shaker-structure interactions at resonance. Alternatively, this work developed a shaker input that is quick and simple to conduct. It also drives a targeted modal amplitude beyond that achievable by impacts which overload the drive point accelerometer.

The basic concept is to excite the structure with a sine wave at a single frequency whose amplitude is shaped by a short triangle function such that all of the input energy is concentrated near the target modal frequency.

$$v_i(t) = a(t) \sin(2\pi f_c t) \quad (23.1)$$

where $v_i(t)$ is the voltage sent to the shaker amplifier, f_c is the center frequency, and $a(t)$ is the time history of the triangle function, see Fig. 23.4.

The frequency content of $v_i(t)$ is shown in Fig. 23.5. The maximum amplitude occurs at f_c and the first local minima occurring at f_{fm} Hz above and below this value. By taking the Fourier transform of a triangle wave, the ramp up (or down) time of the triangle function, t_r , is calculated to be inversely related to f_{fm} as in the following.

$$t_r = \frac{1}{f_{fm}} \quad (23.2)$$

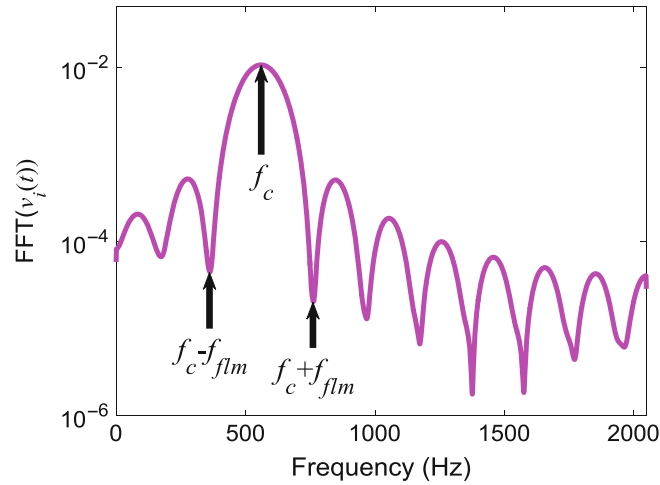


Fig. 23.5 Shaker input spectrum

Table 23.3 Shaker input parameters

Mode	f_c (Hz)	f_{fm} (Hz)
7	128	50
8	169	50
11	560	200
14	974	200

Thus, the shape of this spectrum can be specifically tailored by independently selecting the center frequency and the location of the first local minima. These values can then be used with (23.1) and (23.2) to create the voltage signal that is sent to the shaker.

In this work, f_c was selected to be the approximate linear natural frequency of the targeted mode and f_{fm} was chosen based on the target mode's linear natural frequency and damping and the proximity of nearby modes. This work did not include an exhaustive evaluation of the ramifications of various values of f_{fm} , and the values of f_{fm} for the four nonlinear modes were chosen by the authors' judgement. Table 23.3 contains the input function parameters used in the testing of all the nonlinear modes.

Exciting the structure via the shaker voltage signal described above would ideally focus the force input in a similar fashion to produce essentially a scaled version of Fig. 23.5. However, the force measured by the load cell is influenced both by the shaker input and the response of the test hardware. Thus, the force spectrum is not as smooth as the voltage spectrum and can actually have significant dips near the resonances. Since the goal of this shaker testing is to concentrate the input energy near the resonance, the shaker voltage is updated with measurements in order to maximize the response of the targeted mode. This is accomplished using the transfer function between voltage signal from (23.1) and the corresponding force measured during a test where $v_i(t)$ was the input to the shaker.

$$G_{vf}(\omega) = \frac{F(\omega)}{V_i(\omega)} \quad (23.3)$$

where $F(\omega)$ is the measured force from the experiment. A desired force spectrum, $F_D(\omega)$, can be created by scaling $V_i(\omega)$ until its minima at $f_c \pm f_{fm}$ are at approximately the same value as those in $F(\omega)$. Then, dividing $F_D(\omega)$ by the transfer function from (23.3) results in an updated shaker voltage signal spectrum, $V_u(\omega)$.

$$V_u(\omega) = \frac{F_D(\omega)}{G_{vf}(\omega)} \quad (23.4)$$

The inverse Fourier transform of $V_u(\omega)$ produces an updated time signal, $v_u(t)$, that is subsequently used as the shaker amplifier input voltage for a second test, improving the energy concentration at the targeted resonance. The nonlinear parameters for the targeted modes are extracted from the data from this second updated experiment. This process is summarized in Fig. 23.6.

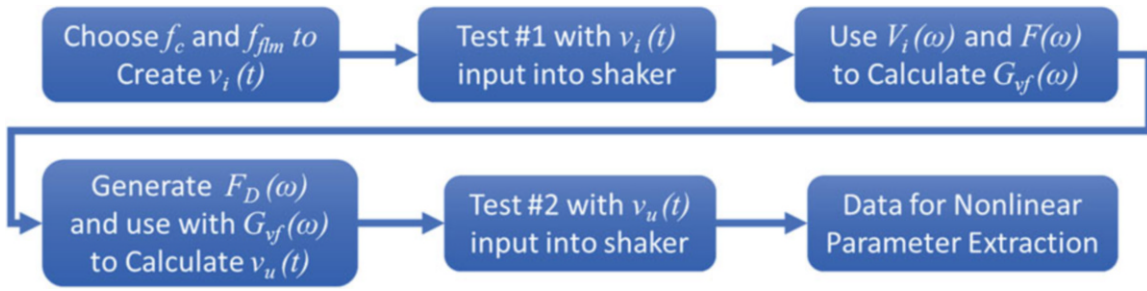


Fig. 23.6 Shaker input creation and updating flowchart

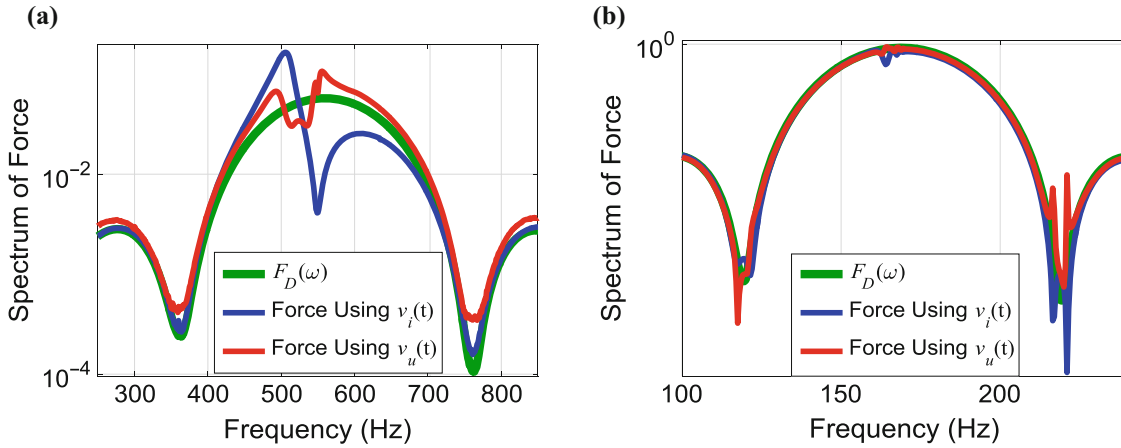


Fig. 23.7 Shaker input updating effectiveness; (a) least effective replication of desired force and (b) most effective replication of desired force

Note the transfer function is a linear operator, so this updating process has limited efficacy due to the nonlinearities in the test object. However, for this work, this updating process performed sufficiently well to concentrate the input energy at the resonance. Fig. 23.7 shows two examples of this updating process. The left plot shows an instance where the updating process made significant improvement, but still struggled to replicate the desired force spectrum. The right plot shows an example where the updating process resulted in a force spectrum very similar to the desired.

Generally, this method was able to produce higher modal responses than that achieved with a hammer without overloading the drive point or beam tip accelerometers. Fig. 23.8 shows a comparison of the maximum modal responses achieved using either shaker or hammer excitation. For modes 7 and 8, the shaker was able to excite the CPB an order of magnitude higher than the hammer before overloading the beam tip accelerometer. Conversely, for mode 14 the limiting factor for the shaker input was the stinger buckling. Overall, the shaker was found to better excite targeted modes.

23.3 Modal Filtering

To develop a nonlinear pseudo-modal model, our approach requires the structural response be separated into the individual modal responses. This requires some type of filter that can transform multiple sensor measurements into modal coordinates. Once these modal responses are calculated, the nonlinear parameters can be identified. Previous work showed that the modal filter embedded in the SMAC algorithm generally suppresses non-target modes better than other methods [1]. The following describes in greater detail the SMAC modal filter.

We desire a modal filter such that

$$\bar{\Psi}^{-T} \bar{x} = q_i \tag{23.5}$$

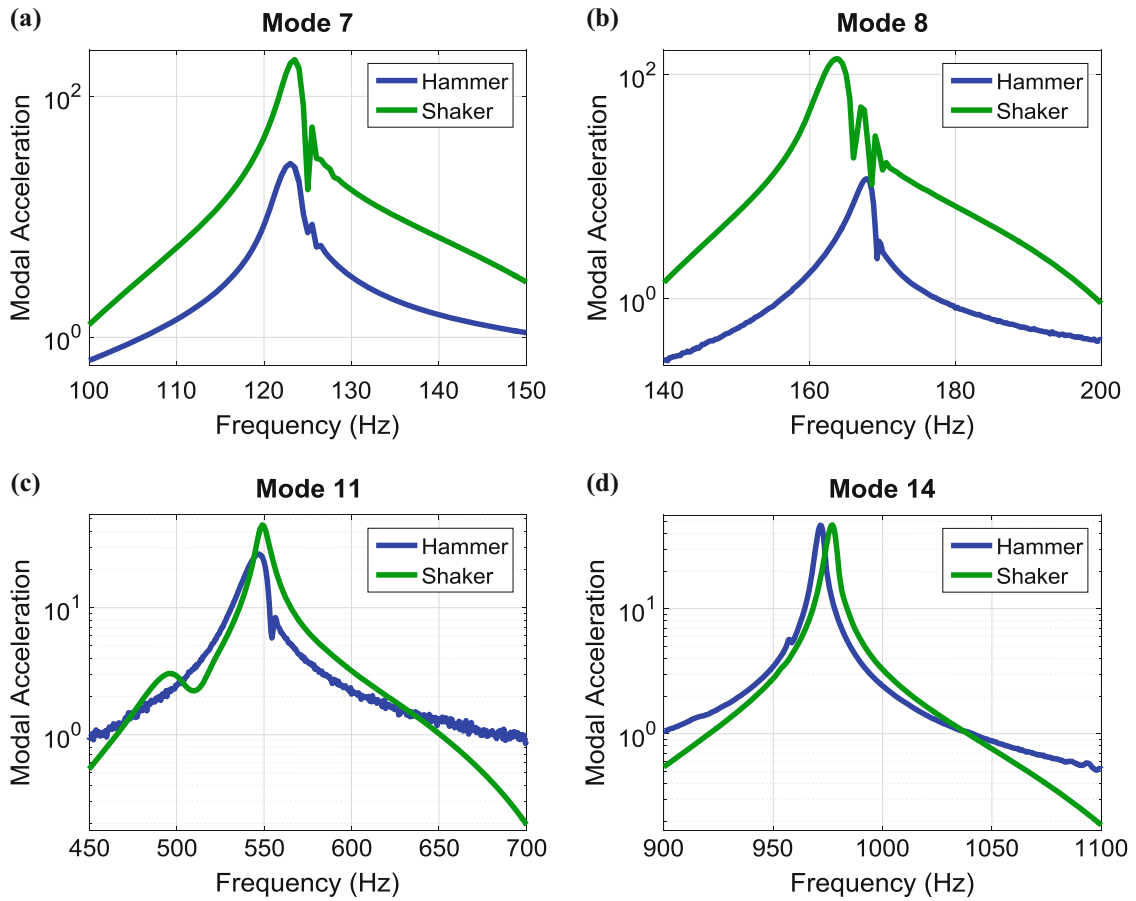


Fig. 23.8 (a–d) Maximum modal responses without overloading accelerometers from shaker and hammer

where q_i is the i^{th} modal DOF, column vector $\bar{\mathbf{x}}$ contains measured responses, and $\bar{\Psi}$ is the vector of weights transforming the measured responses to the modal response. The SMAC modal filter [3] obtains this vector by operating directly on the FRFs. If one employs (23.5) in the frequency domain and divides by the input force, then

$$\bar{\Psi}^{-T} \bar{\mathbf{H}}_x = H_{qi} \quad (23.6)$$

where $\bar{\mathbf{H}}_x$ is now a vector of measured FRFs and H_{qi} is an analytically calculated SDOF FRF with an estimate of the frequency and damping of the target mode and is given by

$$H_{qi} = \frac{\varphi_{dp,i}}{\omega_{ni}^2 - \omega^2 + j2\zeta_i\omega_{ni}\omega} \quad (23.7)$$

where $\varphi_{dp,i}$ is the drive point shape value for the i^{th} mode. Columns for every frequency line of interest are included in $\bar{\mathbf{H}}_x$ and H_{qi} creating a matrix of $\bar{\mathbf{H}}_x$ and a vector of the analytical FRF $\bar{\mathbf{H}}_{qi}$. Transposing (non-conjugate) and isolating the modal filter on the left side yields

$$\bar{\Psi} = \bar{\mathbf{H}}_x^{\text{T}+} \bar{\mathbf{H}}_{qi} \quad (23.8)$$

where the superscript $+$ represents the pseudo-inverse. Hence, the SMAC modal filter is obtained with the measured FRFs and an analytical SDOF FRF constructed using the linear estimate of the natural frequency, damping, and drive point shape of the target mode.

23.4 Nonlinear Model

This section describes the pseudo-modal approach to capture the nonlinearities in the CPB. This approach assumes each mode can be modeled with a single degree of freedom system as a modal coordinate. Each modal degree of freedom is linked to ground with a linear spring and damper. In order to capture the nonlinearity, one adds nonlinear spring and damper elements in parallel with the linear spring and damper as seen in Fig. 23.9.

There are many methods to model/parameterize the nonlinearity. Reference [1] compares the capabilities of the Iwan, FREEVIB, and Restoring Force Surface (RFS) methods to capture the nonlinear response of the CPB in a foam-filled configuration. The RFS method is utilized for this work with the nonlinear spring and damping forces parameterized with cubic polynomials.

The RFS method has been extensively researched and refined with several permutations, see reference [4] for an extensive synopsis of the past variances and applications. The foundation of RFS is in the Newtonian equation of motion:

$$\ddot{q}(t) + F_r(q(t), \dot{q}(t)) = F(t) \quad (23.9)$$

where $F_r(q, \dot{q})$ represents the damping and stiffness forces (called the restoring forces) and $F(t)$ is the excitation force. Assuming the acceleration and excitation force are measured, then at every time instant, the restoring force is also known. We write F_r as in the following:

$$F_r(q(t), \dot{q}(t)) = c_0\dot{q}(t) + c_1|\dot{q}(t)|\dot{q}(t) + c_2\dot{q}^3(t) + k_0q(t) + k_1|q(t)|q(t) + k_2q^3(t) \quad (23.10)$$

where c_1 , c_2 , k_1 , and k_2 are constants. Since c_0 and k_0 are already known from the low level modal tests (see Table 23.2), (23.9) is rearranged to

$$\begin{bmatrix} |\dot{q}|\dot{q} & \dot{q}^3 & |q|q & q^3 \end{bmatrix} \begin{bmatrix} c_1 \\ c_2 \\ k_1 \\ k_2 \end{bmatrix} = F - \ddot{q} - c_0\dot{q} - k_0q \quad (23.11)$$

where the time-dependency has been omitted for clarity. Equation (23.11) can be expressed as

$$\mathbf{P} \begin{bmatrix} c_1 \\ c_2 \\ k_1 \\ k_2 \end{bmatrix} = \bar{\mathbf{U}} \quad (23.12)$$

Fig. 23.9 Schematic of SDOF for RFS modal coordinate

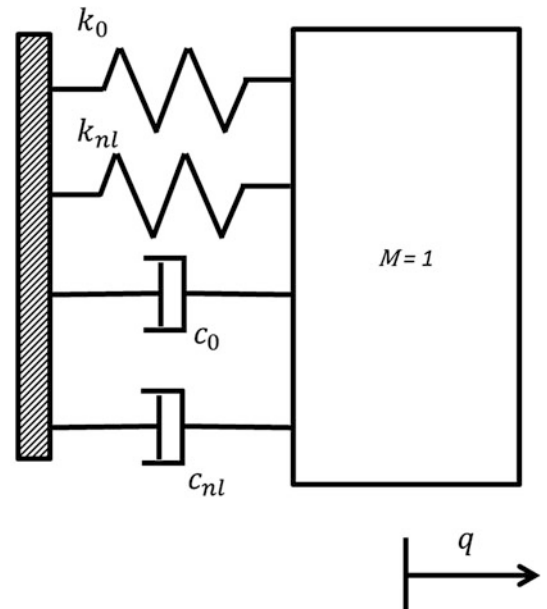


Table 23.4 Damping and stiffness coefficients

Mode	c_0	c_1	c_2	k_0	k_1	k_2
7	4.77	2.6	-1.95	6.48E + 05	-9.15E + 07	3.77E + 10
8	6.61	3.17	-3.28	1.15E + 06	-2.86E + 08	1.92E + 11
11	23.9	318	-834	1.24E + 07	-2.05E + 10	1.54E + 14
14	27.8	-188	811	3.77E + 07	-6.16E + 09	8.41E + 13

where \mathbf{P} and $\bar{\mathbf{U}}$ are processed measurements with a row for each time sample. We obtained the best results by taking the Fourier transform of $\bar{\mathbf{U}}$ and each column of \mathbf{P} giving

$$\mathbf{P}_F \begin{bmatrix} c_1 \\ c_2 \\ k_1 \\ k_2 \end{bmatrix} = \bar{\mathbf{U}}_F. \quad (23.13)$$

Note that in order to yield real coefficients, \mathbf{P}_F must be reconfigured to.

$$\mathbf{P}_F = \begin{bmatrix} \text{real}(\mathbf{P}_F) \\ \text{imaginary}(\mathbf{P}_F) \end{bmatrix}. \quad (23.14)$$

$\bar{\mathbf{U}}_F$ must be similarly restructured. Pre-multiplying $\bar{\mathbf{U}}_F$ by the pseudo-inverse of \mathbf{P}_F results in the least-squares estimate for c_1 , c_2 , k_1 , and k_2 as in (23.15).

$$\begin{bmatrix} c_1 \\ c_2 \\ k_1 \\ k_2 \end{bmatrix} = \mathbf{P}_F^+ \bar{\mathbf{U}}_F. \quad (23.15)$$

Note that acceleration, velocity, and displacement must all be known (estimated or measured). For this work, acceleration was obtained from the modal filtered measured accelerations and the other two states were estimated by integrating in the frequency domain.

The identification procedure described above was performed on the four identified nonlinear modes, and the results are provided in Table 23.4.

23.5 Results and Observations

To evaluate the effectiveness of the pseudo-modal model extracted as described above, a truth test was conducted where the CPB was excited from DOF 31349Y via a 0.3 s chirp (i.e. a very fast sine sweep) from 50 to 1400 Hz. This DOF was chosen since it excited three of the four nonlinear modes. The amplitude of the sweep was varied in order to maximize the response of each nonlinear mode without exceeding the maximum voltage limit of any accelerometer.

The pseudo-modal model with all 14 modes (6 rigid body, 4 linear and 4 nonlinear) was excited with simulated modal forces corresponding to the measured excitation signal from the truth test. The calculated modal responses were transformed back to the physical DOF via the linear mode shape matrix extracted from the low level test. These responses were compared against the measured data from the truth test in Figs. 23.10 and 23.11 which show the drive point response in the frequency and time domains, respectively. Note that the line labeled ‘‘Linear’’ is the response of a modal model which used only the linear parameters of all 14 modes.

The 31349Y drive point DOF does not excite mode 8 and thus there is no corresponding response in either of these figures. Additionally, the colored boxes in Fig. 23.11 approximately correspond to the maximum response of the indicated modes. Figs. 23.10 and 23.11 show that the nonlinear model offers an improved results over the linear model.

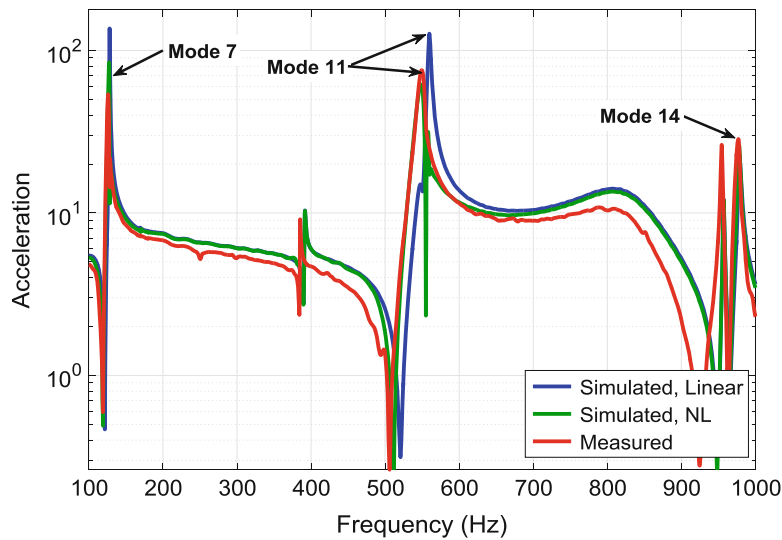


Fig. 23.10 Truth test simulation results, FFT of the drive point response for input DOF 31349Y

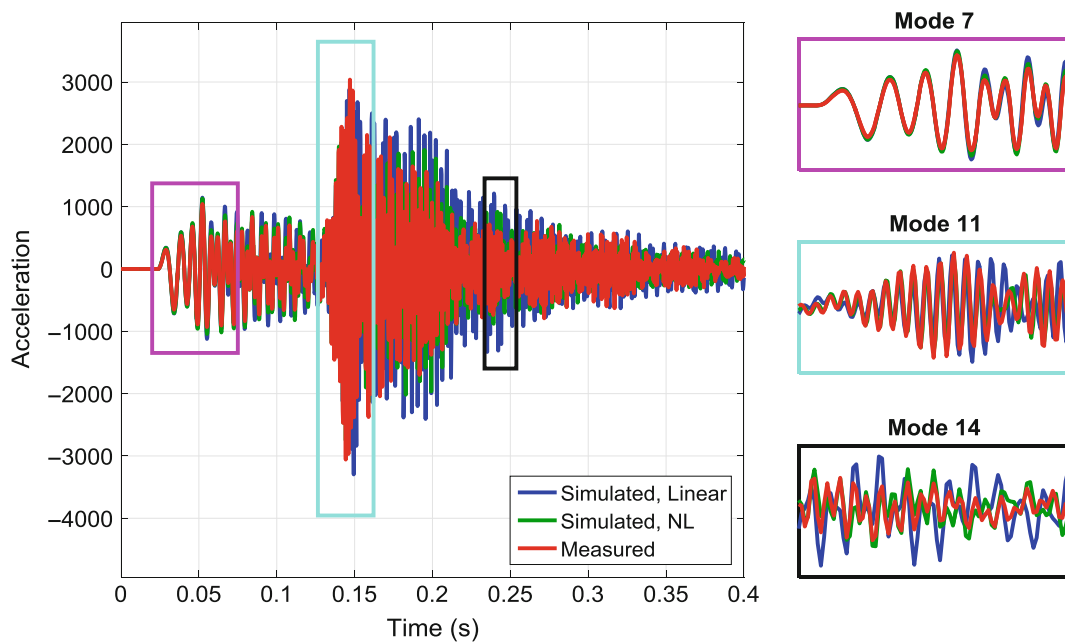


Fig. 23.11 Truth test simulation results, time domain drive point response for input DOF 31349Y

23.6 Discussion

The shaker inputs were able to drive the CPB to a much higher modal response than the hammer without overloading any accelerometers by concentrating the excitation energy near a targeted modal frequency. There are multiple benefits to this. The first is that the input spectrum can be tailored to minimize nearby resonances, enhancing the desired single mode response. The purer the modal response, the greater the accuracy of the extracted nonlinear parameters. The second advantage is that higher response amplitudes can be achieved for a given sensitivity range of accelerometers, allowing for the characterization of nonlinearities over a larger amplitude range. Thus a more accurate nonlinear model can be generated and a greater understanding of the hardware can be attained.

Although imperfect, the truth test results demonstrate that using simple cubic polynomials was an effective method for representing damping and stiffness nonlinearities of the test hardware. These models are easy to understand and were considered adequate for this work. Higher order polynomials could achieve a better fit to the measured data, but they also introduce worse conditioning for the pseudo-inverse of \mathbf{P} in (23.15). The engineer may decide what polynomial order is adequate.

A disadvantageous feature of the polynomial nonlinear model is that, outside the amplitude range in which its coefficients were fit, the polynomial tends toward infinity (either positive or negative). This can cause the simulation to become unstable and give erroneous results. Therefore, the pseudo-modal with the nonlinear damping and stiffness represented by polynomials should only be used to interpolate and not for extrapolation.

23.7 Conclusions

This work showed the capability of using a pseudo-modal model to capture nonlinearities of a real structure using cubic polynomials for the stiffness and damping forces. The coefficients for these polynomials were extracted from data measured during shaker tests. A method was developed to create inputs for these shaker tests specifically tailored to concentrate the excitation energy around a target mode. This allowed for the excitation of individual modes to amplitudes greater than that achievable by impact testing while not overloading any accelerometers. Additionally, concentrating the energy around a target mode increased the efficacy of the modal filter, creating a purer modal response from which to extract nonlinear parameters. A truth test consisting of a chirp from 50 to 1400 Hz showed that the nonlinear pseudo-modal model effectively captured the nonlinear dynamics seen in the CPB and matched the measured data better than a linear model.

Acknowledgement Notice: This manuscript has been authored by Sandia Corporation under Contract No. DE-AC04-94AL85000 with the U.S. Department of Energy. The United States Government retains and the publisher, by accepting the article for publication, acknowledges that the United States Government retains a non-exclusive, paid-up, irrevocable, world-wide license to publish or reproduce the published form of this manuscript, or allow others to do so, for United States Government purposes.

References

1. Mayes, R.L., Pacini, B.R., Roettgen, D. R.: A modal model to simulate typical structural dynamic nonlinearity. Presented at the 34th International Modal Analysis Conference, Orlando, FL, paper #121 January 2016
2. Hensley, Daniel P., Mayes, Randy L.: Extending SMAC to multiple references. Proceedings of the 24th International Modal Analysis Conference, Orlando, FL, pp. 220–230, January 2006
3. Mayes, R.L., Johansen, D.D.: A modal parameter extraction algorithm using best-fit reciprocal vectors. Proceedings of the 16th International Modal Analysis Conference, Santa Barbara, CA, pp. 517–521, February 1998
4. Gaëtan, K., Worden, K., Vakakisc, F.A., Golinval, J.C.: Past present, and future of nonlinear system identification in structural dynamics. *Mech. Syst. Signal Process.* **20**, 505–592 (2006)